Development 130, 1645-1657

doi:10.1242/dev.00395

A *hedgehog* homolog regulates gut formation in leech (*Helobdella*)

Dongmin Kang[1,*], Françoise Huang[1], Dongling Li[2,†], Marty Shankland[2], William Gaffield[3] and David A. Weisblat[1,‡]

[1]Department of Molecular and Cell Biology, 385 LSA, University of California, Berkeley, CA 94720-3200, USA
[2]Section of Molecular Cell and Developmental Biology, Institute for Cellular and Molecular Biology, University of Texas, Austin, Texas 78712, USA
[3]Western Regional Research Center, ARS, USDA, Albany, CA 94710, USA
*Present address: Department of Biological Sciences, Stanford University, CA 94305, USA
†Present address: Cancer Research Laboratory, University of California, Berkeley 94720,USA
‡Author for correspondence (e-mail: weisblat@uclink4.berkeley.edu)

Accepted 17 January 2003

SUMMARY

Signaling by the *hedgehog* (*hh*)-class gene pathway is essential for embryogenesis in organisms ranging from *Drosophila* to human. We have isolated a *hh* homolog (*Hro-hh*) from a lophotrochozoan species, the glossiphoniid leech, *Helobdella robusta*, and examined its expression by reverse transcription polymerase chain reaction (RT-PCR) and whole-mount in situ hybridization. The peak of *Hro-hh* expression occurs during organogenesis (stages 10-11). No patterned expression was detected within the segmented portion of the germinal plate during the early stages of segmentation. In stage 10-11 embryos, *Hro-hh* is expressed in body wall, foregut, anterior and posterior midgut, reproductive organs and in a subset of ganglionic neurons. Evidence that *Hro-hh* regulates gut formation was obtained using the steroidal alkaloid cyclopamine, which specifically blocks HH signaling. Cyclopamine induced malformation of both foregut and anterior midgut in *Helobdella* embryos, and no morphologically recognizable gonads were seen. In contrast, no gross abnormalities were observed in the posterior midgut. Segmental ectoderm developed normally, as did body wall musculature and some other mesodermal derivatives, but the mesenchymal cells that normally come to fill most of the coelomic cavities failed to develop. Taken with data from *Drosophila* and vertebrates, our data suggest that the role of *hh*-class genes in gut formation and/or neural differentiation is ancestral to the bilaterians, whereas their role in segmentation evolved secondarily within the Ecdysozoa.

Key words: *hedgehog*, *Helobdella robusta*, Gut formation, Cell signaling

INTRODUCTION

The gene *hedgehog* (*hh*) was originally identified in *Drosophila* as a segment polarity gene (Heemskerk and DiNardo, 1994; Ingham et al., 1991). Subsequently, *hh*-class genes have been found in many organisms including chordates [*Amphioxus*, zebrafish, frog, chick, mouse and human (reviewed by Shimeld, 1999)] and mollusc [limpet (Nederbragt et al., 2002)]. In addition to their role in patterning larval segments in fly (Nusslein-Volhard and Wieschaus, 1980), HH-class proteins have been shown to play key roles in intercellular signaling during limb development in fly and vertebrates (Vervoort, 2000), neural tube patterning in chordates (McMahon, 2000; Patten and Placzek, 2000; Shimeld, 1999), gut formation in fly and vertebrate, cancer in vertebrates (Toftgard, 2000), cell survival and cell proliferation (Britto et al., 2000) (see also Hammerschmidt et al., 1997; Ingham and McMahon, 2001; McMahon, 2000).

The consensus HH protein contains a secreted domain (NH_2-terminal fragment; HH-N) that functions in extracellular signaling pathways and a C-terminal domain (HH-C) that is involved in intracellular post-translational autoprocessing and covalent attachment of cholesterol (Chuang and Kornberg, 2000; Lee et al., 1994). Sequence alignments among known *hh* homologs reveal that the HH-N domains are usually more conserved than HH-C domains.

Current molecular phylogenies support the organization of all or most extant bilaterian animals into 3 ancient clades, Deuterostomia, Ecdysozoa and Lophotrochozoa (Adoutte et al., 2000; Aguinaldo et al., 1997). Until recently, all of the *hh*-class genes reported in the literature were from members of the former two clades. The recent discovery that a *hh*-class gene from the limpet *Patella vulgata* (Lophotrochoazoa) is expressed along the ventral midline has been interpreted as supporting the dorsoventral axis inversion theory and as supporting a role for *hh*-class genes in neural patterning (Nederbragt et al., 2002), but functional tests of these ideas are yet to be reported. Thus, the question of which aspect(s) of *hh*-class gene function are conserved between Lophotrochozoans and the other two groups remain of interest, both for deducing the nature of early bilaterian ancestors and for understanding the evolution of body plans by modification of developmental mechanisms.

For example, in *Drosophila* embryos *hh* plays a pivotal role in segmentation. The *hh* gene is co-expressed with *engrailed*

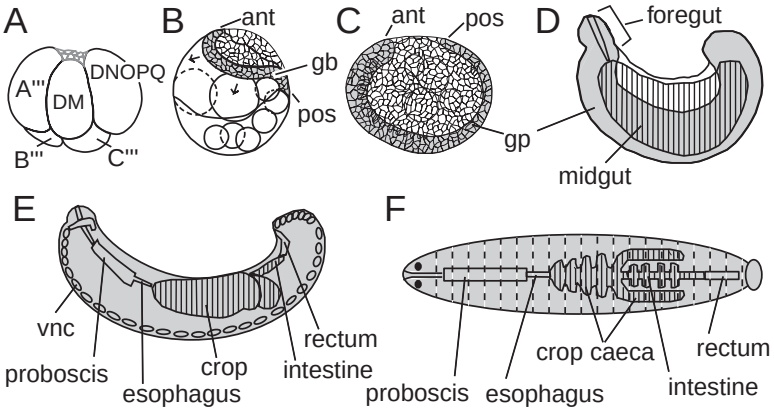

Fig. 1. Schematic depiction of relevant stages of *Helobdella* development. (A-E) Lateral views with animal pole at top and anterior to left; (F) dorsal view. (A) Stage 4b (10 hours AZD); cells DNOPQ and DM arise from macromere D′ at third cleavage and give rise to the teloblasts that generate segmental mesoderm and ectoderm. Macromeres A‴, B‴ and C‴ are endodermal precursor cells. Micromeres are evident at the animal pole. (B) Early stage 8 (~61 hours AZD); DM and DNOPQ have cleaved to generate the full complement of 10 teloblasts (circles, only 8 are shown in the drawing) plus additional micromeres. Each teloblast produces a column of segmental founder cells (blast cells); ipsilateral bandlets merge, forming left and right germinal bands (gb; shaded; only left gb is visible in this lateral view), which are covered by micromere-derived epithelium stretching over the animal pole (net pattern). As blast cells are added to their posterior (pos) ends, the germinal bands elongate and move ventrovegetally (arrows) and coalesce from anterior (ant) to posterior (pos) along the ventral midline, forming the germinal plate (gp), accompanied by the expansion of the micromere-derived epithelium. (C) Late stage 8 (~94 hours AZD); the completed germinal plate (shaded) extends from anterior to posterior, defining the ventral territory of the embryo. (D) Mid stage 10 (~155 hours AZD); during stage 10, segmental tissues arise from the proliferation and differentiation of cells within the germinal plate (shaded), the edges of which gradually expand dorsally and meet at the dorsal midline, closing the definitive body tube. Macromeres, teloblasts and supernumerary blast cells have fused into a syncytial yolk cell (hatched) that constitutes the midgut; foregut arises largely from micromere progeny (the micromere-derived epithelium is omitted for clarity). (E) Early stage 11 (~172 hours AZD). By this stage, the foregut has generated distinct proboscis and esophagus, while the midgut has given rise to crop, intestine and rectum; segmental tissues are well-differentiated, including ganglia within the ventral nerve cord (vnc). (F) Late stage 11 (~195 hours AZD); crop caeca are well-differentiated [adapted from Kang et al. (Kang et al., 2002)].

(*en*) in the posterior compartment of each nascent segment, and the secreted HH protein functions to specify the fates of cells in the adjoining anterior compartment in a concentration-dependent manner (Heemskerk and DiNardo, 1994; Lee et al., 1992). Later in *Drosophila* development, the *hh* and *en* genes are also expressed in identical compartment-specific patterns in the imaginal discs (Tabata and Kornberg, 1994). An *en*-class gene has been described in glossiphoniid leeches, a group of segmented lophotrochozoans (phylum Annelida, class Hirudinea). But while leech-*en* is expressed during segmentation and neurogenesis (Lans et al., 1993; Wedeen and Weisblat, 1991), more recent work suggests that it does not play a direct role in segmentation (Shain et al., 1998) and that the cells that express leech *en* are not required to specify the fates of cells in the remainder of the segment (Seaver and Shankland, 2001). These observations raise the question as to whether *hh*-class genes are expressed coincident with *en*-class genes in the leech embryo, and, if so, how that expression might relate to segmentation.

Here, we report the identification and characterization of a *hh* homolog (*Hro-hh*) from the glossiphoniid leech, *Helobdella robusta*. *Hro-hh* is expressed zygotically in gut and some other tissues, but *Hro-hh* RNA was not detected in the cells that express *Hro-en* during segmentation. In addition, we found that bath-application of cyclopamine, a known blocker of *hh* signaling in vertebrates (Helms et al., 1997; Incardona et al., 1998; Incardona et al., 2000) induced malformation of foregut, anterior midgut and coelomic mesenchyme in *Helobdella*, but had no apparent effect on the segmental patterning of mesoderm and ectoderm. Along with data on the function of *hh*-class genes in vertebrates and insects, our results support a scenario in which the ancestral role of *hedgehog* family genes in bilaterian animals was associated with gut formation and/or neural differentiation, rather than segmentation.

MATERIALS AND METHODS

Embryos

Helobdella robusta embryos were obtained from a laboratory breeding colony (Shankland et al., 1992) or from specimens collected in a minor tributary of the American River in Sacramento, California. For some experiments, embryos were obtained from a separate breeding colony, founded with individuals collected from the mouth of Shoal Creek in Austin Texas. This second population closely resembles *H. robusta* from Sacramento, both morphologically and as judged by comparisons of nuclear gene sequences (see below), but exhibits significant divergence as judged by differences in mitochondrial gene sequences (A. E. Bely, personal communication). Embryos were cultured at 23°C in HL saline (Blair and Weisblat, 1984). The embryonic stages are as defined previously (Weisblat and Huang, 2001), or for greater precision, in terms of the time elapsed after zygote deposition (AZD).

The relevant aspects of glossiphoniid leech development are illustrated in Fig. 1. During cleavage (stages 1-7), 5 bilateral pairs of stem cells (M, N, O/P, O/P and Q teloblasts), 3 macromeres (A‴, B‴ and C‴) and 25 micromeres are formed. Teloblasts undergo repeated, highly unequal divisions to generate columns (bandlets) of founder cells (blast cells) for segmental mesoderm and ectoderm in an anterior-to-posterior progression (stages 5-8). The five bandlets on each side of the embryo join together in parallel to form the germinal bands, which then coalesce from anterior to posterior along the ventral midline into the germinal plate (stage 8); the segmented nervous system, nephridia, epidermis, and musculature differentiate from the germinal plate during stages 9-11. Micromeres contribute definitive progeny to non-segmented tissues such as the supraesophageal ganglion and the foregut of the adult leech, and also a squamous epithelium that covers the germinal bands and the intervening prospective dorsal territory during gastrulation (Fig. 1) (Bissen and Weisblat, 1989; Weisblat et al., 1984). The midgut epithelium forms by cellularization of a syncytial yolk cell (SYC), that arises by the stepwise fusion of the A‴-C‴ macromeres, teloblasts (after they have completed blast cell production), and supernumerary blast cells (Fig. 1) (Desjeux and Price, 1999; Isaksen et al., 1999; Liu et al., 1998; Nardelli-Haefliger and Shankland, 1993).

For cell lineage tracing, selected teloblasts or proteloblasts (stages 4-7) were pressure-injected with a solution of tetramethylrhodamine dextran amine (RDA, Molecular Probes Inc.) at a final concentration of 50 mg/ml in 0.2 N KCl, with 1% Fast Green to permit visual monitoring of the injections (Weisblat et al., 1980). Injected embryos were cultured to stages 9-10, then fixed and processed for in situ hybridization as described below. Prior to fixation, all embryos at mid stage 9 or beyond were relaxed in a solution of 8% ethanol in 4.8 mM NaCl, 1.2 mM KCl, 10 mM $MgCl_2$ (relaxant HL saline). Some embryos were stained with Hoechst 33258 (1 μg/ml) to visualize cell nuclei.

Isolation of *Hro-hh*

An initial fragment of *Hro-hh* was amplified from an *H. robusta* cDNA library (embryonic stages 7-10; Stratagene) by the polymerase chain reaction (PCR), using the following degenerate primers:

Hro-hh1: 5′-GCGTIACIGARRGNWGRGAYGARGA-3′ [VTE(SG)(WR)DED]

Hro-hh2: 5′-ACCCARTCRAAICCIGCYTCNACNGC-3′ [VEAGFDWV]

The PCR reaction mixture contained 50 mM KCl, 10 mM Tris, pH 9.0, 2.5 mM $MgCl_2$, 0.1% Triton X-100, 0.2 mM each dNTP, 0.8 mM each primer, 1 μl *H. robusta* cDNA library (~10^{10} pfu/ml; Stratagene), and 1 unit Taq polymerase (Perkin-Elmer) in a 50 μl volume. For the amplification, we employed a 3-step 'touchdown' protocol: 5 cycles of 94°C for 1 minute, 53°C for 1 minute, 72°C for 1 minute; 10 cycles of 94°C for 1 minute, 50°C for 1 minute, 72°C for 1 minute; then 20 cycles of 94°C for 1 minute, 48°C for 1 minute, 72°C for 1 minute. The amplified DNA was purified from an agarose gel using Gel Extraction Kit (Qiagen) and cloned into pGEM T easy vector (Promega).

The 150 bp *Hro-hh* sequence was amplified and labeled with [^{32}P]dCTP from cloned pGEM T easy plasmid by PCR. We used this probe to screen an *H. robusta* cDNA library (stages 7-10; Stratagene). Phage plating and hybridization were carried out according to manufacturer's instructions with minor modifications. Hybridization was performed at 45°C in 6× SSC, 5× Denhardt's solution, 0.5% SDS, 500 μg/ml herring sperm DNA and 50% deionized formamide. The filters were washed in 2× SSC, 0.5% SDS at 65°C for 1 hour and in 0.1× SSC, 0.1% SDS for 3 hours. pBlueScript SK(–) phagemids were excised in vivo according to the manufacturer's instructions. A plasmid (pHrohh) containing 3.49 kb *Hro-hh* fragment was sequenced. This sequence (GenBank accession number AF517943) was confirmed by RT-PCR from cDNA prepared from total RNA as described below.

Independently, another *hh*-class gene fragment was isolated by degenerate PCR from the *Helobdella* population collected in Austin, Texas, using primers corresponding to nucleotides 934-952 of *Hro-hh* in the forward direction and nucleotides 1060-1077 in the reverse direction, as follows:

hh5: 5′-ACNGARGGNTGGGAYGAAG-3′

hh3: 5′-CCARTCRAANCCNGCTTC-3′

From the 107 nucleotide sequence obtained, there was only a single synonymous change (position 1053). In keeping with this high degree of sequence identity, the same probe was used for in situ hybridization experiments on both types of embryos and the results obtained were indistinguishable.

Developmental RT-PCR

Total RNA samples were prepared from *H. robusta* embryos at selected stages with RNA Wiz (Ambion) according to the manufacturer's instructions, using 40 embryos for each sample. The RNA samples were added to solutions containing 1× reverse transcription buffer (Gibco), 3.33 mM DTT, 0.33 mM dNTP, 3.33 μM random decamer (Ambion), and 200 Units reverse transcriptase (Gibco). The mixture was incubated at 42°C for 50 minutes and the resultant first strand cDNA (30 μl) was stored at –20°C. PCR conditions were as described by the manufacturer of ampliTaq Polymerase (Perkin-Elmer Cetus, Norwalk, CT) except that 3 μl of cDNA template were used in 50 μl of reaction mixture.

To amplify an *Hro-hh*-specific fragment (96 bp in length), a pair of PCR primers was designed as follows:

hh-F: 5′-GAAACTCATCCAGAAGACTCC-3′

hh-R: 5′-TCTAGCCAACATCCCATACTTG-3′

PCR conditions for amplifying the *Hro-hh* fragment were: 1 minute at 94°C, 1 minute at 60°C, and 1 minute at 72°C for 5 cycles, followed by 1 minute at 94°C, 1 minute at 58°C, and 1 minute at 72°C for 17 cycles. A 15 μl aliquot of each sample was removed after 22 cycles and the remaining material underwent 5 more cycles of amplification.

As an internal standard to adjust for differences in efficiency of RNA extraction between samples, a 488 bp fragment of 18S rRNA was amplified in parallel to each *Hro-hh* sample. For this purpose, and to attenuate the signal obtained from the abundant rRNAs, bona fide and non-extending 18S primers (competimers; Ambion) were used in a 3:7 ratio, respectively. PCR conditions for amplifying the 18S rRNA fragment were: 1 minute at 94°C, 1 minute at 58°C and 1 minute at 72°C for 1 minute for 5 cycles, followed by 1 minute at 94°C, 1 minute at 56°C, and 1 minute at 72°C for 10 cycles. A 15 μl aliquot of each sample was removed after 15 cycles and the remaining material underwent 5 more cycles of amplification.

To quantitate PCR products, each sample was run out in a 2% agarose gel and stained with ethidium bromide. Band intensity was measured with an Alphaimager (Alpha Innotech Corp.) using Alphaease (v3.3b) program.

In situ hybridization

In situ hybridization was performed using a digoxigenin-labeled RNA probe with some modifications of methods described previously (Harland, 1991; Nardelli-Haefliger and Shankland, 1992). Sense and antisense probes (each of 3.6 kb length) were obtained by T7 and T3 in vitro transcription (MEGAscript kit, Ambion) using linearized pHrohh (cut with *Bam*HI to generate the sense probe, and with *Sal*I to generate the antisense probe) and subsequently hydrolyzed into shorter fragments (~300 bp) in an alkaline solution (Cox et al., 1984).

Early embryos (stage 1-8) were fixed in 4% formaldehyde in PBS (130 mM NaCl, 10 mM phosphate buffer, pH 7.4) for 1 hour, then permeabilized by a 5-minute incubation with 50 μg/ml proteinase K (Gibco); late embryos (stages 9-11) were fixed as described above for 30 minutes, then treated for 25 minutes in 0.5 mg/ml Pronase E (Sigma).

Hybridization was carried out overnight at 59°C in a 1:1 mixture of deionized formamide and 5× SSC, 0.2 mg/ml tRNA, 0.1 mg/ml heparin, 1× Denhardt's solution, 0.1% Tween 20 and 0.1% Chaps. Alkaline phosphatase (AP)-conjugated anti-digoxigenin Fab fragments (Roche) were added to a dilution of 1:5000 in 1× PBS, 0.1% Tween 20 for late embryos. To remove unhydrolyzed probe, embryos were treated with RNase A (Sigma; 50 μg/ml for 1 hour for early embryos and 5 μg/ml for 30 minutes for late embryos) at 37°C. Alkaline phosphatase (AP)-conjugated anti-digoxigenin Fab fragments (Boehringer-Mannheim) were added (1:2000 in 1× PBS, 10% normal goat serum, 0.1% Tween 20, 0.2% Triton X-100 for early embryos; 1:5000 in 1× PBS, 0.1% Tween 20 for late embryos) and the color reaction was carried out using nitro blue tetrazolium chloride/5-bromo-4-chloro-3-indoyl-phosphate (NBT/BCIP; Roche) by standard procedures. Intact embryos were dehydrated in ethanol and propylene oxide, followed by infiltration with plastic embedding medium (Poly/Bed 812; Polysciences).

Cyclopamine treatment

Cyclopamine was obtained from *Veratrum californicum* as described previously (Gaffield et al., 1986) and was diluted to a final concentration of 10 μM, 5 μM and 1 μM in HL saline (from a stock solution of 10 mM in ethanol). Experimental embryos (early or mid stage 8; 60-68 AZD) were cultured in cyclopamine for 3-6 days

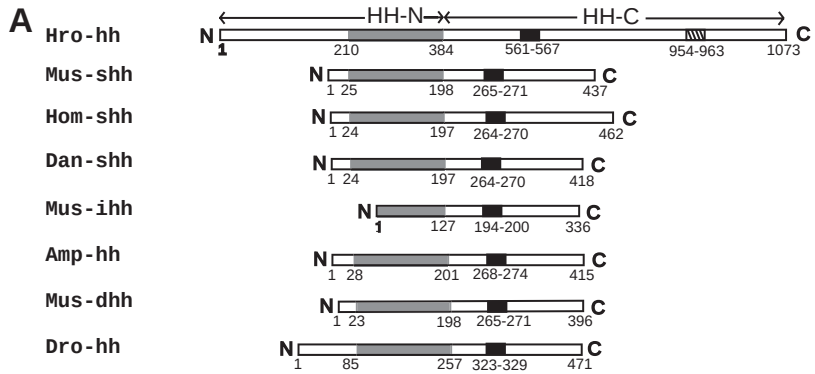

Fig. 2. *Hro-hh* is an *hh* homolog. (A) Domain alignment of HH-homologs in leech (Hro-hh; accession number AF517943), mouse (Mus-shh, Q62226; Mus-ihh, P97812; Mus-dhh, Q61488), human (Hom-shh, Q15465), zebrafish (Dan-shh, A49426), *Amphioxus* (Amp-hh, CAA74169) and fruitfly (Dro-hh, L02793): secreted HH amino terminus (HH-N, gray box); within the less well conserved carboxy-terminal fragments (HH-C), putative autoprocessing sequence motifs (PASM, black box) and the cell division sequence motif (CDSM, hatched box) in *Hro-hh* are indicated. (B) Alignment of HH-Ns, including the available sequence from a mollusc, *Patella vulgata* (Pat-hh, AF435840). (C) Alignment of PASMs in HH-Cs. Gray shading in B and C indicates conserved residues. shh, sonic hedgehog; ihh, Indian hedgehog; dhh, desert hedgehog.

(sibling controls were cultured in HL saline with 0.1% ethanol). Treated embryos were then examined morphologically.

Histology and microscopy

For closer examination than was possible in whole mount, some embryos were dehydrated through a series of graded alcohols to 95% and then embedded in glycolmethyacrylate resin (JB-4; Polysciences, Inc) according to the manufacturer's instructions. Embedded specimens were sectioned with glass knives on a Sorvall MT2-B microtome. Sections were mounted on glass slides and stained with Hoechst 33258 (1 μg/ml).

In our hands, the AP reaction product obtained by in situ hybridization is not stable in JB-4 embedding resin. So to examine such embryos in section, the selected specimens were dehydrated and embedded in epoxide embedding resin (Poly/Bed 812; Polysciences) following the manufacturer's instructions, and sectioned at ~10 μm thickness with glass knives using a Sorvall MT2-B microtome or at ~100 μm thickness using hand-held razor blades. Sections were mounted on glass slides under coverslips in a non-fluorescing medium (Fluoromount; BDH Laboratory Supplies, Ltd.), and photographed with Nomarski optics (Zeiss Axiophot) or observed with confocal microscope (MRC 600; Bio-Rad) in 0.1 μm optical sections.

Whole embryos or sections were viewed with DIC optics (Zeiss

Axiophot or Nikon E800 microscope) and photographed using Ektachrome 160 film (Kodak) or with a 'Spot' CCD camera (Diagnostics, Inc.). Live embryos were paralyzed in relaxant HL saline prior to photography.

RESULTS

A *hedgehog* homolog from the leech *Helobdella robusta*

Degenerate PCR primers were designed by comparing the conserved regions of *hh* homologs from *Drosophila* and various vertebrate species (Echelard et al., 1993). These primers amplified a 150 bp fragment of a putative *hh*-class gene from a genomic library and from a cDNA library representing stages 7-10 *H. robusta* embryos, (but not from a stage 1-6 cDNA library). This fragment was cloned, sequenced and then used to screen a cDNA library. From ~120,000 plaques, one positive phage was isolated, and its insert was sequenced. This sequence was confirmed by independent PCR amplification from first strand cDNAs representing stage 9-10 embryos. The *Hro-hh* cDNA encodes a predicted 3219 bp (1073 amino acids) open reading frame (ORF) which is flanked by 186 bp of 3′ UTR and 75 bp of 5′ UTR. The amino and carboxy termini of the encoded HRO-HH polypeptide are well conserved with respect to those of known HH homologs (Fig. 2). This led us to conclude that we had cloned the entire coding sequence of this *Hro-hh* transcript.

HRO-HH contains two apparent cleavage sites, CGPG in the amino region and GCF in the carboxy region that are conserved among HH-class polypeptides and are predicted to generate a secreted peptide (HRO-HH-N; Fig. 2A) consisting of 175 amino acids, compared with 173 amino acids in *Drosophila* and 174 amino acids in human and mouse SHH (Fig. 2B). In other organisms, HH-N is involved in extracellular signaling pathways (Chuang and Kornberg, 2000) and it seems likely that this function is conserved in HRO-HH-N.

In other organisms, HH-C is important for autoproteolysis of the HH propeptide and for covalently attaching cholesterol to the carboxyl terminus of HH-N. HRO-HH-C is less well conserved than HRO-HH-N, based on amino acid sequence comparison with other HH-class proteins (Fig. 2) and is longer than any other known HH-C peptides, but a region resembling the proposed active site motif (PASM) of HH-C peptides [including the invariant T and H residues required for autoproteolysis (Lee et al., 1994)] was also found in HRO-HH-C at residues 561-567 (Fig. 2A,C).

We also note the presence in HRO-HH-C of a putative cell division sequence motif (CDSM) not found in other HH proteins. The consensus motif ([ND]-C-[TES]X[DE][EDTS][DE], where X is a spacer of 1-8 amino acids) exists in the v-myc and c-myc oncoproteins, CDC25, and other proteins thought to carry out one of the required steps in the cell division competency cascade of deactivating a cell division repressor (Figge and Smith, 1988). The presence of this motif in *Hro-hh* (**D**KT**C**DS**I**D**SE**, residues 954-963; Fig. 2A), suggests that HRO-HH-C may also be involved in intracellular signaling related to the control of cell division.

To investigate the relationships between *Hro-hh* and previously described *hh*-class genes, we used ClustalX 1.81 to construct an unrooted phylogram, comparing that portion of the conserved HH-N domain for which sequences were available for all species of interest (Fig. 3). The best supported tree grouped *Hro-hh* with *hh* from *Drosophila* and *Patella*, separate from the deuterostome *hh*-class genes, in accord with the accepted metazoan phylogenetic tree based on rRNA sequence (Adoutte et al., 2000; Aguinaldo et al., 1997).

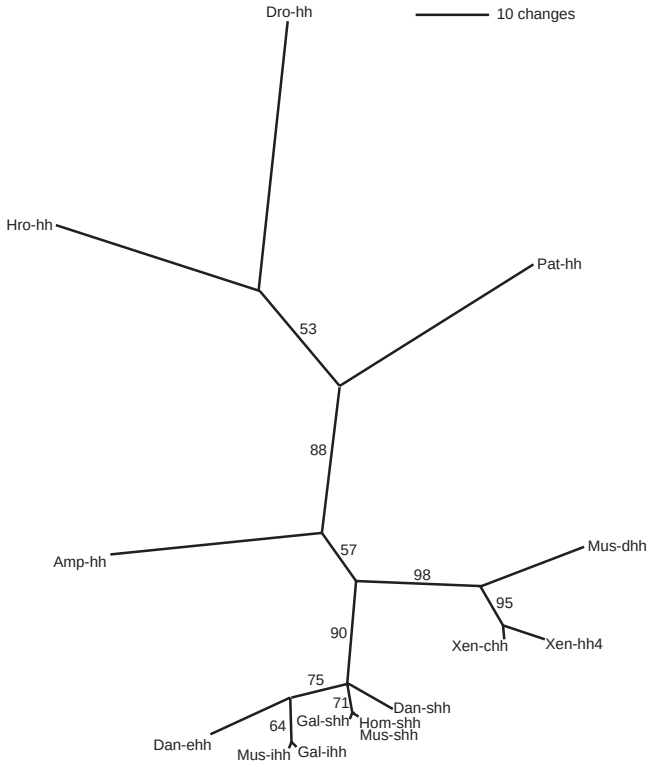

Fig. 3. Unrooted phylogram for *hh*-class genes recreates the accepted evolutionary relationships among protostomes (Dro-hh; Hro-hh and Pat-hh) and deuterostomes (all others). Well-supported branches are indicated by numbers (percentage of 100-replicate bootstrap trials). Abbreviations and accession numbers as in Fig. 1, plus chick (Gal-ihh, Q98938 and Gal-shh, Q91035), *Xenopus* (Xen-chh, Q91610 and Xen-hh4, Q91611) and another zebrafish gene (Dan-ehh, Q98862). See text for details.

Expression of *Hro-hh* is zygotic and peaks during organogenesis

Because the relatively small number of embryos available precludes the routine application of northern blot analysis for most genes in *H. robusta*, we used semi-quantitative RT-PCR to obtain an initial developmental expression profile for *Hro-hh*. For this purpose, 18S ribosomal RNA was used as an internal standard, to control for variations in the efficiency of RNA extraction and reverse transcription reaction (see Materials and Methods). By this assay (Fig. 4), *Hro-hh* is an exclusively zygotic transcript. Transcripts were not detected in dissected oocytes or in zygotic stages prior to stage 8, which is many hours after all the teloblasts have been generated and are actively making blast cells. Transcript levels increase through late stage 10, which correlates with the major period of organogenesis, and then decline slowly in stage 11, as the embryo completes its transformation into a juvenile leech.

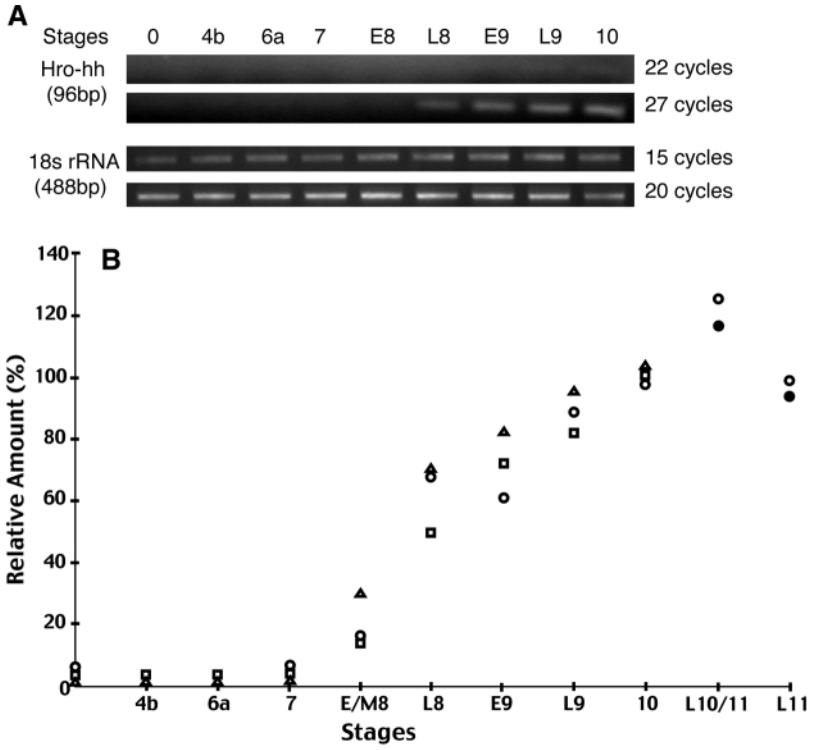

Fig. 4. Semiquantitative RT-PCR demonstrates late zygotic transcription of *Hro-hh*. (A) Digital images of ethidium bromide-stained agarose gels. Fragments of *Hro-hh* and 18S rRNA were amplified in separate reactions carried out in parallel. (B) Amount of *Hro-hh* mRNA during development, relative to stage 10 (100%). At each stage, the intensity of the *Hro-nos* band was normalized against the 18S rRNA fragment (see Materials and Methods for details). Each reaction sample contained template cDNA equivalent to 4 embryos at the stage indicated [stage 4b ~10 hours AZD, stage 6a ~19 hours AZD, stage 7 ~40 hours AZD, early/mid stage 8 (E/M8) ~65 hours AZD, late stage 8 (L8) ~88 hours AZD, early stage 9 (E9) ~112 hours AZD, late stage 9 (L9) ~140 hours AZD, stage 10 ~150 hours AZD, late stage 10/stage 11(L10/11) 170~185 AZD, late stage 11(L11) ~195 AZD]. Squares indicate the data obtained from the gels shown in (A); circles and triangles represent data obtained starting with independent sets of embryos; black circles show the data from independent PCR.

Hro-hh is expressed in various tissues, including foregut and midgut

In situ hybridization was used to characterize *Hro-hh* expression in specific tissues and cells (Figs 5-7). Expression was first observed in stage 8 embryos, consistent with the results of RT-PCR. But, in contrast to expectations based on the role of *hh* in *Drosophila* segmentation, *Hro-hh* mRNA was detected in the anteriormost, unsegmented (prostomial) region (Fig. 5A,B) and not in the segmenting germinal plate at this stage (Fig. 5A,C). Even extensively overstained embryos showed no signal other than diffuse staining presumed to be background in the segmental tissues (data not shown) until later stages when segmentally iterated organs and tissues were differentiating (described below).

By the end of stage 8, two distinct sets of cells expressing *Hro-hh* could be distinguished (Fig. 5C,D): one at the anterior end of the germinal plate marked what we surmise to be the prospective stomodeum; the other lay beneath it, next to the SYC, at the junction between the future foregut (proboscis and esophagus) and anterior midgut. This staining demarcates the region in which the proboscis will form, and in progressively older embryos, the *Hro-hh* staining pattern expanded to encompass the full length of the developing proboscis (Fig. 5E,G; Fig. 6A,B). Expression in the proboscis finally disappeared during stage 11 (Fig. 6H).

The proboscis of glossiphoniid leeches is a tri-radiate, muscular tube (see Fig. 7A) that is everted during feeding to pierce host or prey tissues and suck out blood or soft body parts. This process is aided by secretions from ductules arising in the salivary glands and running the length of the proboscis. As illustrated in Fig. 1, the proboscis occupies the everted position during the early stages of its morphogenesis (stages 9 and early 10), and then assumes the inverted position (late stage 10 and beyond).

Hro-hh expression was largely confined to the inner layer of the developing proboscis, proximal to the lumen (Fig. 5E,G). Beginning in stage 9, staining was also seen in a ring of external tissue surrounding the base of the proboscis (Fig. 5E-G). This ring is apparently transformed into the epithelial lining of the oral opening once the proboscis has inverted (Fig. 6A,B). *Hro-hh* expression continued within the proboscis through early stage 11 (Fig. 6A,B), and transverse sections of such embryos revealed that the lumen proximal staining was in presumptive radial muscle cells throughout the length of the proboscis (Fig. 6C,D). Within the posterior portion of the proboscis, staining was also seen in presumptive longitudinal muscle cells, more distal to the lumen (Fig. 5F, Fig. 6D).

In addition to the expression in the foregut described above, *Hro-hh* expression was evident in cells associated with the midgut. Beginning in late stage 8 and continuing into stage 9, *Hro-hh* was seen in faint, segmentally iterated, transverse stripes at the interface of the germinal plate and the SYC (prospective midgut; Fig. 5H). These stripes appeared only after segmental morphology was established, and were associated with the developing gut wall at the dorsal edge of the intersegmental septa (Fig. 5I). During stage 9, most of these stripes fade, but five persist and become stronger during stage 10, so that by stage 11 *Hro-hh* staining was seen in a series of five rings around the posterior midgut derivatives: one at the boundary between crop and intestine; one near the boundary of the intestine and rectum; and three around the rectum (Fig. 6B,G). Also by stage 11, a speckled pattern of staining was evident at the surface of the crop (Fig. 6B,F,G). By mid-stage 11, much of the expression appears to have disappeared, except for the rings of presumptive muscle associated with the intestine and rectum (Fig. 6H,I).

Staining was also seen in cells at the lateral edges of the germinal plate during stage 9 (Fig. 5H), and during stage 10,

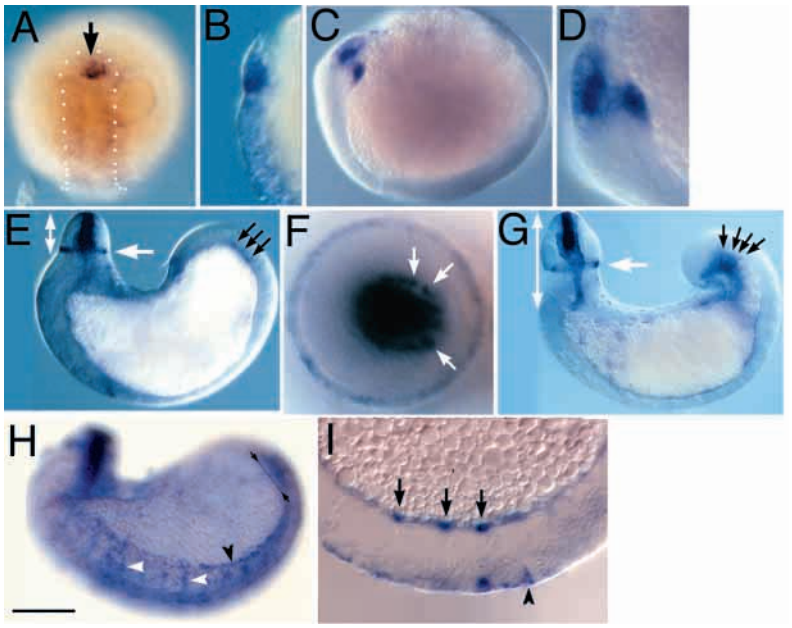

Fig. 5. Early expression of *Hro-hh* in gut tissues, but not in germinal plate, prior to the establishment of segmental boundaries. Photomicrographs of embryos processed by in situ hybridization for *Hro-hh*. In these and all subsequent illustrations, embryos are shown in lateral views, with anterior to left and ventral down, unless otherwise stated. (A) Anteroventral view of a stage 8 embryo (~78 hours AZD) showing the partially formed germinal plate (dotted outline); transcripts (arrow) occur at the anterior, micromere-derived end of the germinal plate, from which prostomial tissues and proboscis arise, but not in the more posterior, teloblast-derived region that will form segmental ectoderm and mesoderm. (B) Lateral view of the same embryo, at higher magnification. (C,D) An embryo at early stage 9 (~100 hours AZD), showing the presence of two distinct groups of cells expressing *Hro-hh* at the anterior end of the germinal plate; there are still no transcripts visible within the segmental portion of the germinal plate. (E) By early stage 10 (~135 hours AZD), the proboscis is starting to differentiate in the everted position. *Hro-hh* transcripts are present in the central core of the proboscis (extent indicated by double-headed arrow), in a ring of cells defining the future oral opening (white arrow) and in transverse bands of cells at the posterior end of the SYC, corresponding to posterior midgut (black arrows). Relatively weak expression is also observed in the prospective esophagus, between the circumoral ring and the yolk cell. (F) A higher magnification view of the embryo shown in E, looking down along the longitudinal axis of the foregut and focussed at the level of the circumoral ring. In this view, *Hro-hh*-expressing longitudinally oriented fibers (arrows) appear as dots surrounding the core of the proboscis. (G) At mid stage 10 (~145 hours AZD), transcripts are clearly present throughout the extent of esophagus and proboscis (doubleheaded arrow), in the circumoral ring (white arrow), and in the rectum (black arrows), which is becoming morphologically distinct from the crop. Patches of *Hro-hh* expression are also visible at the surface of the anterior portion of the crop. (H) An embryo at the same age as that in E, in which the color reaction was allowed to proceed longer. This image is focused on the lateral edge of the germinal plate. *Hro-hh* transcripts are visible along the edge of the germinal plate (black arrowhead) and in transverse segmentally iterated bands (white arrowheads). (I) Parasagittal section (ventral is down, posterior to right) through the posterior segments of an embryo at a similar stage to that shown in H (paired arrows in H). In three segments, precursors of the rings of stained rectal muscle (arrows) lie at the dorsal edge of the intersegmental septa. Staining is also present in the body wall, with a clear boundary at the boundary between the prospective midbody and caudal sucker (black arrowhead). Scale bar: A, 150 μm; B 75 μm; C,E,G,H, 100 μm; D, 50 μm; F, 25 μm; I, 20 μm.

in the male and female reproductive tissues (Fig. 6A,E) and throughout most of the definitive epidermis of the body wall. The epidermal staining was more intense in the posteriormost midbody segments, and absent at the ends of the embryo, corresponding to the presumptive anterior and posterior suckers (Fig. 5I, Fig. 6A,G). Finally, by stage 11, *Hro-hh* expression was also seen in a small number of segmentally iterated cell bodies in the ganglia of the ventral nerve cord (Fig. 6A,C).

Identity and embryonic origins of cells expressing *Hro-hh* in proboscis

A prominent structural feature of the proboscis is an extensive array of radial muscles (Fig. 7A,B), whose contractions open the lumen of the proboscis to draw in food; their actions are opposed by a thick, interwoven band of circumferential muscles situated roughly midway along the radius of the proboscis (Fig. 7A,B). Nuclei of the radial muscles are situated within the ring of circumferential muscle. Outside this ring, the space between the radial muscles is occupied by relatively sparse sets of longitudinal muscles and a large number of ductules that carry salivary gland secretions to the tip of the proboscis (Fig. 7B).

Thus, given the observed staining patterns, the prime candidates for cells expressing *Hro-hh* near the lumen of the developing proboscis are the radial muscles and/or circumferential muscles, while the longitudinally oriented fibers near the outer surface in the posterior portion of the proboscis correspond to longitudinal muscles. We have previously established that presumptive circumferential muscles of the proboscis arise from micromeres c‴ and dm′ (Huang et al., 2002). Careful examination of sectioned, in situ-stained embryos in which cell dm′ had been injected with lineage tracer, revealed no doubly labeled cells (Fig. 7G). All the cells colored with the in situ reaction product lay within or outside the ring of tracer-labeled circumferential muscles. From this, we conclude that it is the radial muscles and longitudinal muscles, and not the circumferential muscles, that express *Hro-hh* in the proboscis at this stage.

The embryonic origins of the radial and longitudinal muscles are less clear, but on the basis of our previous results, it seemed that the primary quartet micromeres (a′-d′) and secondary trio micromeres a″ and c″ were good candidates for contributing at least some of these muscles. Consistent with this interpretation, *Hro-hh*-stained embryos in which micromere a″ had been injected with lineage tracer did contain some doubly labeled cells near the core of the proboscis that appear to be radial muscle precursors (Fig. 7H). Embryos in which primary quartet micromeres (a′, b′ and d′) had been injected showed double labeling of some radial muscle precursors, and also of some longitudinal fibers in the outer layers of the proboscis that we assume are presumptive longitudinal muscles (Fig. 7D-F).

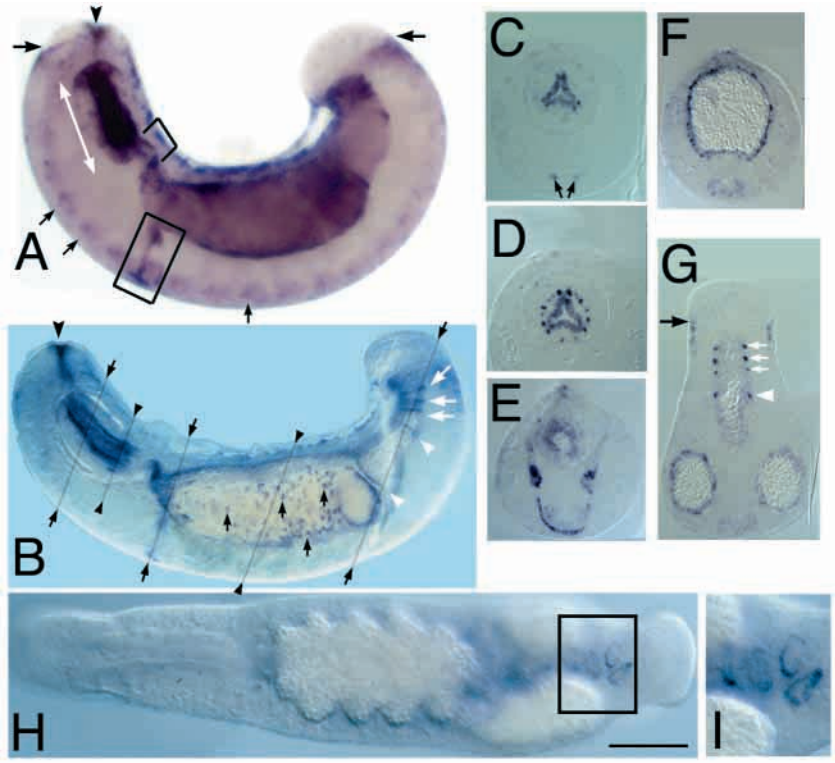

Fig. 6. Later expression of *Hro-hh* in gut, body wall, reproductive tissue and nervous system. (A) Late stage 10 and (B) early stage 11 embryos (~160 and ~180 hours AZD) from two separate hybridization experiments. The embryo shown in B was later sectioned in a roughly transverse orientation. Selected sections, corresponding to the planes indicated by the paired arrows and arrowheads, are shown in C-G. In each embryo, *Hro-hh* transcripts are visible within the oral opening (black arrowhead in A,B), along the inner portion of the proboscis (inverted by this stage; extent indicated by double-headed white arrow in A) and esophagus (bracket in A), in reproductive organs (box in A), around the crop (vertical arrows in B), at the crop-intestine and intestine-rectum boundaries (white arrowheads in B) and rectum (white arrows in B). (A) The staining reaction was carried out for somewhat longer for this embryo, revealing low transcript levels in the ventral nerve cord (small arrows) and in the epidermis except for the future anterior and posterior suckers (black horizontal arrows indicate boundaries). (C) Section through the anterior portion of the proboscis (leftmost paired arrows in B) shows *Hro-hh* transcripts in cells near the tri-radiate lumen of the proboscis, and in a pair of neurons (arrows) in the ventral ganglion. (D) Section through a more posterior portion of the proboscis (left paired arrowheads in B) shows transcripts in a ring of longitudinally oriented fibers. (E) Section through the anterior end of the crop (middle paired arrows in B) reveals transcripts in a U-shaped pattern corresponding to the reproductive organs. (F) Section through the middle of the crop (right paired arrowheads in B) shows transcripts in visceral mesoderm and/or endoderm. (G) Section through the posterior portion of the embryo (rightmost paired arrows in B) shows transcripts in visceral mesoderm and/or endoderm of the posterior crop caeca, in muscles associated with the rectum (white arrowhead and arrows), and in the body wall bordering the posterior sucker (black arrow). (H) In later stage 11 (~190 hours AZD), transcripts are largely confined to four rings of presumptive muscle surrounding the rectum (box), shown at higher magnification in I. Scale bar: 100 μm in A, B,H; 90 μm in C-G; 70 μm in I.

Identity and embryonic origins of cells expressing *Hro-hh* in midgut (crop, intestine and rectum)

The wall of the midgut comprises two closely apposed layers of cells. One, an outer layer of visceral mesoderm arises from the same m blast cells that contribute segmentally repeating mesodermal structures such as body wall and nephridia, is laid down in an anteroposterior progression and expands dorsally with the rest of the germinal plate during stages 9-10. The other layer is endoderm that arises by cellularization of the SYC (Nardelli-Haefliger and Shankland, 1993), under mesodermal influence (Wedeen and Shankland, 1997). The SYC arises by a stepwise series of cell-cell fusions, and thus contains nuclei derived from the macromeres, teloblasts, and supernumerary blast cells (Desjeux and Price, 1999; Liu et al., 1998). Because the two layers of cells are thin and tightly apposed, it is difficult to tell them apart, even using lineage tracer injections. The difficulty is compounded by the fact that the M teloblasts have already fused with the SYC by the time visceral mesoderm forms, so it is not possible to label visceral mesoderm without also labeling the endoderm. The rings of staining in the posterior midgut clearly lay outside the endoderm, and presumably corresponded to M-derived muscles ringing the intestine and rectum. But examination of fortuitous sections through the anterior midgut (prospective crop) suggest that some *Hro-hh* expression was also occurring within the endodermal layer (not shown).

Hro-hh signaling is required for normal gut development

To obtain information regarding the functional significance of *Hro-hh* expression in the developing leech, we examined intact and sectioned stage 10-11 embryos that had been grown from early stage 8 in the presence of cyclopamine, a steroidal alkaloid that inhibits HH signaling in vertebrates (Cooper et al., 1998; Incardona et al., 1998; Taipale et al., 2000). In these experiments, epiboly, germinal plate formation and the differentiation of segmental tissues proceeded in parallel between experimental and control embryos (not shown), but the differentiation of the proboscis and crop were clearly disrupted by cyclopamine (Fig. 8).

In particular, the proboscis was shorter and often failed to invert (Fig. 8A,F,J). The esophagus was much longer and thinner than usual and the crop lacked the narrowing anterior projection normally seen during stages 9-10 (Fig. 8J). The crop caeca that normally become prominent during stages 10-11 were reduced in embryos exposed to 5 μM cyclopamine and absent in those exposed to 10 μM cyclopamine (Fig. 8G,I,K). No morphological abnormalities were detected in intestine or rectum and the intestine produced its own small caeca (Fig. 8I,K).

To further test the specificity of the cyclopamine effects, we examined control and cyclopamine-treated embryos in which selected cells had been injected with cell lineage tracer. Ectodermal lineages in cyclopamine-treated embryos were

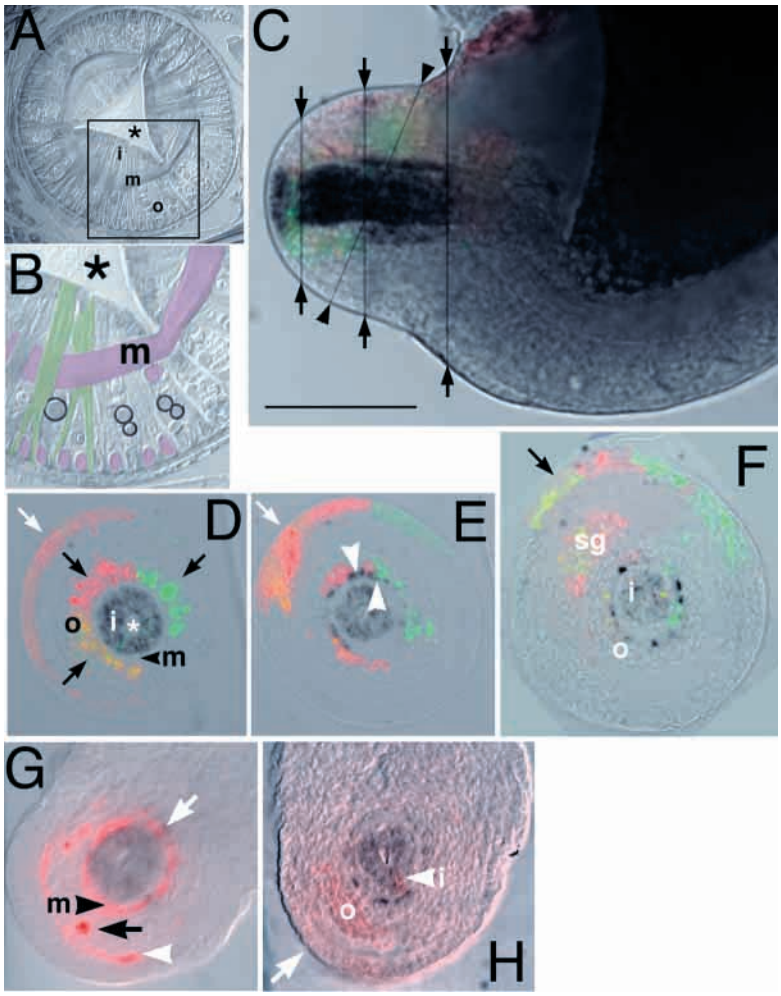

Fig. 7. Cells expressing *Hro-hh* in proboscis arise from specific micromere lineages. (A) Transverse section through the proboscis of an adult *Helobdella*; the triangular lumen (*) is surrounded by an inner ring (i) comprising mainly the thick ends and nuclei of radial muscles, a middle ring (m) comprising circumferential muscles and an outer ring (o) comprising longitudinal muscles and salivary gland ductules. (B) Magnified view of the boxed area in A highlighting two radial muscles (green), a circumferential muscle fiber (m, pink), plus several longitudinal muscle fibers (pink) and ductules (circles). (Labels i and o have been omitted from B for clarity.) (C) Combined bright-field and fluorescence micrographs showing anterior portion of an embryo in which micromeres a′, b′ and d′ had been injected with RDA (red), FDA (green) and both (yellow), respectively, at stage 4 (~8 hours AZD); the embryo was processed for in situ hybridization at early stage 10 (~135 hours AZD), and then sectioned in obliquely transverse orientation through the long axis of the embryo (dorsal is up in all sections). (D) A section through the anterior proboscis (left paired arrows in C). Micromeres a′, b′ and d′ contribute cells to the left dorsal, right dorsal and left ventral quadrants of the outer ring (o) of the proboscis, respectively (black arrows). Other experiments demonstrated that the unlabeled right ventral quadrant contains progeny of micromere c′ (data not shown), consistent with the established symmetry of the clones of these four cells (Nardelli-Haefliger and Shankland, 1993; Smith and Weisblat, 1994; Huang et al., 2002). *Hro-hh* transcripts (dark grey) are localized to the inner ring (i) of presumptive radial muscles surrounding the lumen (white *); some of these cells are co-labeled with FDA (green, partially masked by the in situ signal), indicating their descent from micromere b′. Progeny of a′ are also present in the proboscis sheath (white arrow). Note also the presence of a middle ring (m, black arrowhead) containing neither lineage tracer nor *Hro-hh* transcripts. (E) A section through the mid-portion of the proboscis (middle arrows in C) shows *Hro-hh* transcripts in presumptive longitudinal muscles at the inner edge of the outer ring (white arrowheads); some of these cells appear to co-label with lineage tracer. At this level, all three of the labeled micromeres contribute to the proboscis sheath (white arrow). (F) A section near the posterior end of the proboscis (right arrows in C) includes part of the left side of the supraesophageal ganglion (sg), containing progeny of a′ and d′; at this level, the outer portions of the section pass through definitive epidermis ventrally and a temporary embryonic covering [provisional integument (Weisblat et al., 1984)] dorsally. Progeny of all three micromeres are seen in the epithelium of the provisional integument (black arrow) and in the inner (i) and outer (o) rings of the proboscis, including cells that express *Hro-hh*. (G,H) Obliquely transverse sections (at roughly the level and orientation indicated by the paired arrowheads in C) through an embryo in which micromere dm′ (G) or a″ (H) had been injected with RDA (red) at stage 4 (~10 hours AZD). (G) Progeny of dm′ occupy the middle ring (black arrowhead) of the proboscis, between the inner and outer rings of cells expressing *Hro-hh*. [The seemingly double-labeled cell (white arrow) is an artifact resulting from the thickness and obliquity of the section.] Other dm′ progeny occupy the outer ring (black arrow) and external surface (white arrowhead) of the proboscis. (H) Progeny of micromere a″ contribute to the proboscis sheath (white arrow), and to both the outer (o) and inner (i, white arrowhead) rings of the proboscis. Scale bar: (A,C-H) 50 μm, (B) 30 μm.

indistinguishable from those in controls (Fig. 9A, D, G). In the M lineage, contributions to the provisional integument and ventral nerve cord appeared normal; mesodermal derivatives were also present in the body wall, but the definition and organization of muscle fibers was less clear than in controls. This latter observation correlated with the fact that the germinal plate was very fragile and difficult to dissect in cyclopamine-treated embryos and that the embryos failed to flatten in the DV axis (data not shown).

Cyclopamine also caused defects in the dm' micromere lineage, which normally contributes presumptive circumferential muscles to the proboscis and esophagus (Huang et al., 2002). In normal development, these hoop-like fibers are found from the anterior tip of the proboscis to the anterior end of the crop (Fig. 9A,B). In embryos treated with 5 μM cyclopamine, the circumferential muscles are present in the anterior portion of the proboscis, but absent in the esophagus (Fig. 9D,E). In embryos treated with 10 μM cyclopamine, they are missing from both proboscis and esophagus (Fig. 9G,H). These observations were confirmed by the examination of sectioned embryos (Fig. 8L). The dm′ micromere also contributes a network of fibers that extend throughout the body wall and ramify in the posterior sucker (Huang et al., 2002); these fibers were present at both concentrations tested (Fig. 9C,F,I).

In addition to the foregoing defects, cyclopamine-treated

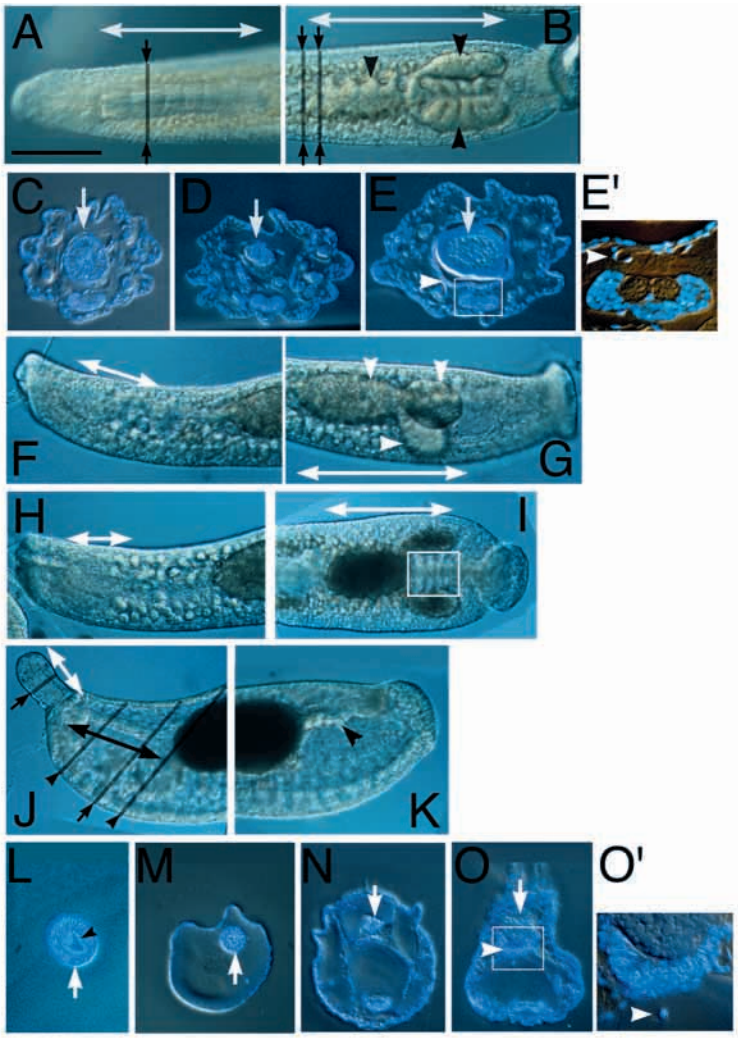

Fig. 8. Cyclopamine treatment disrupts formation of the gut and coelomic mesenchyme (see Materials and Methods for details of treatment). (A,B) Dorsal views of the anterior and posterior portions, respectively, of a control embryo at stage 11 (~200 hours AZD) showing the extent of the proboscis (double headed white arrow in A) and crop (double headed white arrow in B); note the well-differentiated crop caeca (black arrowheads). (C-E) Combined bright-field and fluorescence views of transverse sections (ventral is down; counterstained with Hoechst 33258, blue) through the proboscis (at level of black arrows in A), esophagus (left black arrows in B) and crop (right black arrows in B), of a comparable embryo, at roughly the levels indicated in A and B. Note that the proboscis (arrow in C) has well-defined inner and outer layers separated by a middle layer containing relatively few nuclei and that the visceral mesoderm has spread to form a thin layer of nuclei surrounding the crop [arrowhead in E; E′ is an enlarged view of the box in E showing the ventral blood vessel (arrowhead)]. (F,G) Lateral views of the anterior and posterior portions of a sibling embryo treated with 5 μM cyclopamine. Note the shortened proboscis (double headed white arrow in F) and crop (double headed white arrow in G) and the incomplete differentiation of the crop caeca (white arrowheads in G) relative to those in the control. (H,I) Dorsal views of the anterior and posterior portion of another embryo treated with 5 μM cyclopamine. The proboscis (double headed arrow in H) and crop (double headed arrow in I) are similarly affected, whereas the intestine (box in I) appears normal. (J,K) Lateral views of the anterior and posterior portions of a sibling embryo treated with 10 μM cyclopamine. The proboscis (extent indicated by white double headed arrow in J) is shortened and has failed to invert. The esophagus (extent indicated by black double headed arrow in J) is thin and elongated. The crop lacks even the large posterior caeca, but intestine and rectum are still present (arrowhead in K). (L-O) Views of transverse sections at successively more posterior levels (indicated by black arrows and arrowheads in J) through the proboscis (white arrow in L), esophagus (white arrows in M and N) and crop (white arrow in O), of a comparable cyclopamine-treated embryo. In such embryos, the tri-radiate geometry of the proboscis lumen is less well defined (arrowhead in L) and the middle ring of circumferential muscles is missing (compare L with C). In addition, the coelomic lacunae remain largely devoid of cells (compare N with D) and visceral mesoderm (arrowhead in O) has failed to expand around the crop, but the ventral blood vessel is still present (arrowhead in O′). Scale bar, 100 μm in A, B, F-K; 50 μm in C-E, L-O; 12 μm in E′ and O′.

embryos were more transparent than controls. In normal development, most of the coelom of the leech embryo becomes filled with mesenchyme and other mesodermal derivatives, so that the remaining space is reduced to a relatively narrow system of interconnecting channels (reviewed by Sawyer, 1986) (Fig. 8C-E); this process failed to occur in embryos treated with cyclopamine (Fig. 8M-O). Moreover, in sectioned, cyclopamine-treated embryos, we were unable to recognize any morphogically defined gonads, which appear at this stage in normal embryos as U-shaped structures connected to the ventral ectoderm (see Fig. 6E). In contrast, the ventral blood vessel was still present (Fig. 8E′,O′), which is further evidence for the specificity of the cyclopamine effects.

DISCUSSION

A *hedgehog*-class gene from a lophotrochozoan species

hh-class genes are involved in various aspects of patterning in diverse species. Functional studies have been largely confined to *Drosophila* and vertebrates, which represent two of the three main clades of bilaterally symmetric animals, Ecdysozoa and Deuterostomia, respectively. In the work presented here, we characterized *Hro-hh*, a *hh* ortholog from *Helobdella robusta*, a glossiphoniid leech and a member of the third bilaterian clade, Lophotrochozoa. As in other animals that have been examined, *Hro-hh* is expressed zygotically in a variety of cells and tissues, including subsets of body wall, gonad, nervous system, muscle and gut. We find that *Hro-hh* is expressed by a subset of the mesodermal derivatives of micromere lineages in the foregut and also by mesodermal and possibly endodermal tissues in the midgut; analysis of cyclopamine-treated embryos indicates that *Hro-hh* signaling is required for normal development of the proboscis and anterior midgut, and for mesenchymal tissues that normally come to fill much of the coelom in leeches.

Based on these results, we can try to interpret which elements of the *Hro-hh* expression pattern are responsible for the developmental defects produced by cyclopamine. For

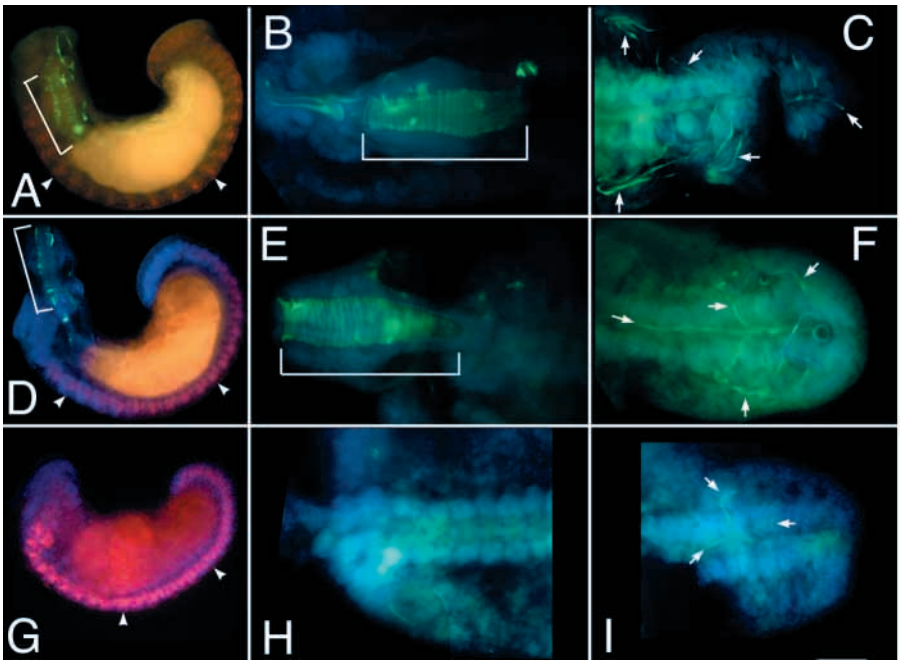

Fig. 9. Cyclopamine treatment disrupts formation of circumferential muscles in proboscis. Fluorescence micrographs of control embryos at early stage 11 (~180 hours AZD; top row) and siblings treated with cyclopamine at 5 μM (middle row) or 10 μM (bottom row). In each embryo, micromere dm′ had been injected with FDA (green) at stage 4 (~10 hours AZD) and an N or OPQ cell with RDA (red) at stage 6a (~20 hours AZD). The left column (A,D,G) shows intact embryos; in each row, the center and right columns are higher magnification views of the anterior (B,E,H) and posterior (C,F,I) of the same embryo, after dissecting the germinal plate from the yolk. In the control embryo, the segmentally iterated pattern of neurons arising from the O, P and Q lineages is visible along the ventral nerve cord (arrowheads in A); dm′-derived circumferential muscles are present throughout the inverted proboscis (bracket in A and B) and a network of dm′-derived fibers (arrows in C) is present in the caudal sucker. In the embryo treated with 5 μM cyclopamine, the segmental pattern of N-derived neurons (arrowheads in D) is not affected; circumferential fibers have formed in the proboscis, though it has failed to invert (bracket D and E) and the posterior fibers (arrows in F) appear as in controls. In the embryo treated with 10 μM cyclopamine, the N-derived neurons (arrowheads in G) and dm′-derived posterior fibers (arrows in I) are still comparable to those in controls, but the dm′-derived circumferential muscles are absent (G,H) and the proboscis is reduced in length. Scale bar: (A,D,G) 100 μm; (B,C,E,F,H,I) 40 μm.

example, it seems likely that the expression of *Hro-hh* by the radial and/or longitudinal muscle fibers of the proboscis is required for the normal development of the circular muscle fibers derived from micromere dm′. The source of the Hro-hh signals that regulate crop morphogenesis and mesenchyme formation is less obvious, but they may originate in the faint stripes of germinal plate expression seen at stage 9 (Fig. 5H).

Though expression of *hh* and *en* are tightly coupled during segmentation in insects, we found no evidence for patterned expression of a leech *hh* gene in the germinal bands or early germinal plate at the time and place where the segmental pattern of *engrailed* expression is first manifest (Wedeen and Weisblat, 1991; Lans et al., 1993), nor is there a clear correlation between the patterns of *hh*- and *en*-class gene expression in the ventral ganglia. Subject to the caveats necessary for any negative result, the apparent dissociation of *en* and *hh* gene expression during leech segmentation is consistent with other studies suggesting that the segmentation processes in *Helobdella* and *Drosophila* are not homologous at the molecular level (Iwasa et al., 2000; Pilon and Weisblat, 1997; Savage and Shankland, 1996; Seaver and Shankland, 2000; Seaver and Shankland, 2001; Shain et al., 1998; Song et al., 2002).

Speculation as to the ancestral role of *hh*-family genes

Given the diverse functions of *hh*-class genes in various organisms, what can we conclude regarding the function of the *hedgehog* gene in the common ancestor of the three main bilaterian clades? The eponymous *hh* was identified as a segment polarity gene in *Drosophila*, and vertebrate *hh*-class genes are critical for patterning limbs and somites. The question is still open (De Robertis, 1997; Dewel, 2000; Collins and Valentine, 2001; Valentine and Collins, 2000), but it seems unlikely to us that the ancestral bilaterian had these particular features, in which case the ancestral *hh* gene could not have functioned in any of those roles.

The first description of a *hh* homolog in Lophotrochozoa has recently been published for the limpet *Patella vulgata*, a gastropod mollusc; its expression in anterior and ventral midline ectoderm of the trochophore larva of that species was interpreted as supporting the dorsoventral axis inversion theory (Nederbragt et al., 2002). Our results, that *Hro-hes* is expressed at low levels throughout the epidermis of the germinal plate of the leech, but with no particular relationship to the developing nerve cord, does not particularly support this interpretation. Of course, *Helobdella* is a derived annelid, so the expression and function of *Hro-hh* may bear little resemblance to those of the ancestral *hh* gene. But the same argument holds for all extant species, including those whose external morphology resembles ancestral forms. Thus, whether the pattern of *hh*-class gene expression seen in the *Patella* trochophore reflects its expression in the urbilateria or an adaptation associated with torsion of the molluscan body plan during gastropod evolution, for example, remains to be seen. In any event, the expression of *hh*-class genes in the nervous system of vertebrates, insects, annelids and (presumably) mollusks suggests that the ancestral *hh* gene(s) may have been involved in some aspect of neural differentiation.

Another candidate function of the ancestral *hh* gene is in gut formation (Pankratz and Hoch, 1995). That the gut is a plesiomorphic trait of bilaterian animals seems beyond dispute, and it has been suggested that signaling between invaginating gut and ectoderm, leading to the formation of

stomodeum/foregut and/or proctodeum/hindgut, was among the first inductive interactions to have evolved (Wolpert, 1994). In chick, *sonic hedgehog* (*shh*, one of 3 *hh*-class genes known in vertebrates) is expressed in the endodermal epithelium throughout much of the gut (Echelard et al., 1993; Roberts et al., 1995; Roberts et al., 1998; Sukegawa et al., 2000). In *Amphioxus*, which arose from a basal branch of the chordate lineage, the one known *hh*-class gene is also expressed in endoderm, among other tissues (Shimeld, 1999). In *Drosophila*, epithelial expression of *hh* is an essential aspect of foregut and midgut formation, but in contrast to chick and *Amphioxus*, the source of the signal is ectodermal rather than endodermal (Hoch and Pankratz, 1996; Pankratz and Hoch, 1995). And now in leech, we find *hh*-class gene expression primarily in mesoderm, the third germ layer, during gut formation.

Similarities between hedgehog signaling pathways may also extend to the level of target genes. The inductive Shh signal regulates the concentric patterning of the surrounding mesenchyme in chick, negatively regulating the differentiation of smooth muscle, in part by activation of *BMP4*, a member of the *TGFβ* superfamily, in those cells (Roberts et al., 1995; Roberts et al., 1998; Sukegawa et al., 2000). Members of the multi-gene *NK-2* family of homeobox genes are also activated by Shh signaling in vertebrates (Barth and Wilson, 1995; Briscoe et al., 1999). In *Amphioxus*, *AmphiBMP2/4* is expressed in hypoblast and endodermal derivatives (Panopoulou et al., 1998), and *AmphiNk2-2* is expressed in anterior nervous system and endoderm (Holland et al., 1998). In *Drosophila*, as in vertebrates, *hh* activates the expression of *TGFß*-related genes (*dpp* and *60A*) in adjacent visceral mesoderm. Moreover, an *NK2*-class gene (*tinman*) is also a downstream target of *hh* signaling in *Drosophila* heart differentiation (Yin and Frasch, 1998). In leech, *Lox10*, an *NK2*-class gene, is known to be expressed in the crop (Nardelli-Haefliger and Shankland, 1993); a *TGFβ*-related gene has been identified, but its expression remains unknown (Isaksen, 1992). Thus, comparison of *hh*-class gene expression and function in a vertebrate (chick), fly and leech reveals some parallels, supporting the hypothesis that signaling in gut formation was an ancestral role for *hh*-class gene in ancient bilaterians, but there are also significant differences. Further work should reveal whether this situation reflects divergence or convergence.

This work was supported by NSF grant IBN 9723114 and NIH grant RO1 GM 60240 to D.A.W., by a fellowship from the Korean Research Foundation to D.K. and by NASA grants NAG2-1349 to S.M.S. and NAG2-1359 to D.A.W. We thank Foster C. Gonsalves for assistance in preparing Fig. 3, and members of the Weisblat and Shankland labs for helpful discussions.

REFERENCES

Adoutte, A., Balavoine, G., Lartillot, N., Lespinet, O., Prud'homme, B. and de Rosa, R. (2000). The new animal phylogeny: reliability and implications. *Proc. Natl. Acad. Sci. USA* **97**, 4453-4456.

Aguinaldo, A. M., Turbeville, J. M., Linford, L. S., Rivera, M. C., Garey, J. R., Raff, R. A. and Lake, J. A. (1997). Evidence for a clade of nematodes, arthropods and other moulting animals. *Nature* **387**, 489-493.

Barth, K. A. and Wilson, S. W. (1995). Expression of zebrafish nk2.2 is influenced by sonic hedgehog/vertebrate hedgehog-1 and demarcates a zone of neuronal differentiation in the embryonic forebrain. *Development* **121**, 1755-1768.

Bissen, S. T. and Weisblat, D. A. (1989). The durations and compositions of cell cycles in embryos of the leech, *Helobdella* triserialis. *Development* **106**, 105-118.

Blair, S. S. and Weisblat, D. A. (1984). Cell interactions in the developing epidermis of the leech *Helobdella triserialis*. *Dev. Biol.* **101**, 318-325.

Briscoe, J., Sussel, L., Serup, P., Hartigan-O'Connor, D., Jessell, T. M., Rubenstein, J. L. and Ericson, J. (1999). Homeobox gene Nkx2.2 and specification of neuronal identity by graded Sonic hedgehog signalling. *Nature* **398**, 622-627.

Britto, J. M., Tannahill, D. and Keynes, R. J. (2000). Life, death and Sonic hedgehog. *BioEssays* **22**, 499-502.

Chuang, P. T. and Kornberg, T. B. (2000). On the range of hedgehog signaling. *Curr. Opin. Genet. Dev.* **10**, 515-522.

Collins, A. G. and Valentine, J. W. (2001). Defining phyla: evolutionary pathways to metazoan body plans. *Evol. Dev.* **3**, 432-442.

Cooper, M. K., Porter, J. A., Young, K. E. and Beachy, P. A. (1998). Teratogen-mediated inhibition of target tissue response to Shh signaling. *Science* **280**, 1603-1607.

Cox, K. H., DeLeon, D. V., Angerer, L. M. and Angerer, R. C. (1984). Detection of mRNAs in sea urchin embryos by in situ hybridization using asymmetirc RNA probes. *Dev. Biol.* **101**, 485-502.

De Robertis, E. M. (1997). Evolutionary biology. The ancestry of segmentation. *Nature* **387**, 25-26.

Desjeux, I. and Price, D. J. (1999). The production and elimination of supernumerary blast cells in the leech embryo. *Dev. Genes Evol.* **209**, 284-293.

Dewel, R. A. (2000). Colonial origin for Emetazoa: major morphological transitions and the origin of bilaterian complexity. *J. Morphol.* **243**, 35-74.

Echelard, Y., Epstein, D. J., St-Jacques, B., Shen, L., Mohler, J., McMahon, J. A. and McMahon, A. P. (1993). Sonic hedgehog, a member of a family of putative signaling molecules, is implicated in the regulation of CNS polarity. *Cell* **75**, 1417-1430.

Figge, J. and Smith, T. F. (1988). Cell-division sequence motif. *Nature* **334**, 109.

Gaffield, W., Benson, M., Lundin, R. E. and Keeler, F. F. (1986). Carbon-13 and proton nuclear magnetic resonance spectra of Veratrum alkaloids. *J. Natural Products* **49**, 286-292.

Hammerschmidt, M., Brook, A. and McMahon, A. P. (1997). The world according to hedgehog. *Trends Genet.* **13**, 14-21.

Harland, R. M. (1991). In situ hybridiazation: An improved whole-mount method for *Xenopus* embryos. *Methods Cell Biol.* **36**, 685-695.

Heemskerk, J. and DiNardo, S. (1994). Drosophila hedgehog acts as a morphogen in cellular patterning. *Cell* **76**, 449-460.

Helms, J. A., Kim, C. H., Hu, D., Minkoff, R., Thaller, C. and Eichele, G. (1997). Sonic hedgehog participates in craniofacial morphogenesis and is down-regulated by teratogenic doses of retinoic acid. *Dev. Biol.* **187**, 25-35.

Hoch, M. and Pankratz, M. J. (1996). Control of gut development by fork head and cell signaling molecules in Drosophila. *Mech. Dev.* **58**, 3-14.

Holland, L. Z., Venkatesh, T. V., Gorlin, A., Bodmer, R. and Holland, N. D. (1998). Characterization and developmental expression of AmphiNk2-2, an NK2 class homeobox gene from Amphioxus. (Phylum Chordata; Subphylum Cephalochordata). *Dev. Genes Evol.* **208**, 100-105.

Huang, F. Z., Kang, D., Ramirez-Weber, F. A., Bissen, S. T. and Weisblat, D. A. (2002). Micromere lineages in the glossiphoniid leech Helobdella. *Development* **129**, 719-732.

Incardona, J. P., Gaffield, W., Kapur, R. P. and Roelink, H. (1998). The teratogenic Veratrum alkaloid cyclopamine inhibits sonic hedgehog signal transduction. *Development* **125**, 3553-3562.

Incardona, J. P., Gaffield, W., Lange, Y., Cooney, A., Pentchev, P. G., Liu, S., Watson, J. A., Kapur, R. P. and Roelink, H. (2000). Cyclopamine inhibition of Sonic hedgehog signal transduction is not mediated through effects on cholesterol transport. *Dev. Biol.* **224**, 440-452.

Ingham, P. W. and McMahon, A. P. (2001). Hedgehog signaling in animal development: paradigms and principles. *Genes Dev.* **15**, 3059-3087.

Ingham, P. W., Taylor, A. M. and Nakano, Y. (1991). Role of the Drosophila patched gene in positional signalling. *Nature* **353**, 184-187.

Isaksen, D. E., Liu, N.-J. L. and Weisblat, D. A. (1999). Inductive regulation of cell fusion in leech. *Development* **126**, 3381-3390.

Iwasa, J. H., Suver, D. W. and Savage, R. M. (2000). The leech hunchback protein is expressed in the epithelium and CNS but not in the segmental precursor lineages. *Dev. Genes Evol.* **210**, 277-288.

Kang, D., Pilon, M. and Weisblat, D. A. (2002). Maternal and zygotic

expression of a nanos-class gene in the leech Helobdella robusta: primordial germ cells arise from segmental mesoderm. *Dev. Biol.* **245**, 28-41.

Lans, D., Wedeen, C. J. and Weisblat, D. A. (1993). Cell lineage analysis of the expression of an engrailed homolog in leech embryos. *Development* **117**, 857-871.

Lee, J. J., Ekker, S. C., von Kessler, D. P., Porter, J. A., Sun, B. I. and Beachy, P. A. (1994). Autoproteolysis in hedgehog protein biogenesis. *Science* **266**, 1528-1537.

Lee, J. J., von Kessler, D. P., Parks, S. and Beachy, P. A. (1992). Secretion and localized transcription suggest a role in positional signaling for products of the segmentation gene hedgehog. *Cell* **71**, 33-50.

Liu, N.-J. L., Isaksen, D. E., Smith, C. M. and Weisblat, D. A. (1998). Movements and stepwise cell fusion of endodermal precursor cells in leech. *Dev. Genes Evol.* **208**, 117-127.

McMahon, A. P. (2000). More surprises in the Hedgehog signaling pathway. *Cell* **100**, 185-188.

Nardelli-Haefliger, D. and Shankland, M. (1992). Lox2 a putative leech segment identity gene is expressed in the same segmental domain in different stem cell lineages. *Development* **116**, 697-710.

Nardelli-Haefliger, D. and Shankland, M. (1993). *Lox10*, a member of the NK-2 homeobox gene class, is expressed in a segmental pattern in the endoderm and in the cephalic nervous system of the leech *Helobdella*. *Development* **118**, 877-892.

Nederbragt, A. J., van Loon, A. E. and Dictus, W. J. A. G. (2002). *Hedgehog* crosses the snail's midline. *Nature* **417**, 811-812.

Nusslein-Volhard, C. and Wieschaus, E. (1980). Mutations affecting segment number and polarity in Drosophila. *Nature* **287**, 795-801.

Pankratz, M. J. and Hoch, M. (1995). Control of epithelial morphogenesis by cell signaling and integrin molecules in the *Drosophila* foregut. *Development* **121**, 1885-1898.

Panopoulou, G. D., Clark, M. D., Holland, L. Z., Lehrach, H. and Holland, N. D. (1998). AmphiBMP2/4, an amphioxus bone morphogenetic protein closely related to Drosophila decapentaplegic and vertebrate BMP2 and BMP4: insights into evolution of dorsoventral axis specification. *Dev. Dyn.* **213**, 130-139.

Patten, I. and Placzek, M. (2000). The role of Sonic hedgehog in neural tube patterning. *Cell Mol. Life Sci.* **57**, 1695-1708.

Pilon, M. and Weisblat, D. A. (1997). A nanos homolog in leech. *Development* **124**, 1771-1780.

Roberts, D. J., Johnson, R. L., Burke, A. C., Nelson, C. E., Morgan, B. A. and Tabin, C. (1995). Sonic hedgehog is an endodermal signal inducing Bmp-4 and Hox genes during induction and regionalization of the chick hindgut. *Development* **121**, 3163-3174.

Roberts, D. J., Smith, D. M., Goff, D. J. and Tabin, C. J. (1998). Epithelial-mesenchymal signaling during the regionalization of the chick gut. *Development* **125**, 2791-2801.

Savage, R. M. and Shankland, M. (1996). Identification and characterization of a hunchback Orthologue, Lzf2, and its expression during leech embryogenesis. *Dev. Biol.* **175**, 205-217.

Sawyer, R. T. (1986). *Clitellate Reproduction and Phylogenetic Affinities*. Oxford, UK: Clarendon Press.

Seaver, E. C. and Shankland, M. (2000). Leech segmental repeats develop normally in the absence of signals from either anterior or posterior segments. *Dev. Biol.* **224**, 339-353.

Seaver, E. C. and Shankland, M. (2001). Establishment of segment polarity in the ectoderm of the leech Helobdella. *Development* **128**, 1629-1641.

Shain, D. H., Ramirez-Weber, F.-A., Hsu, J. and Weisblat, D. A. (1998). Gangliogenesis in leech: Morphogenetic processes leading to segmentation in the central nervous system. *Dev. Genes Evol.* **208**, 28-36.

Shankland, M., Bissen, S. T. and Weisblat, D. A. (1992). Description of the Californian leech Helobdella robusta, new species, and comparison with Helobdella triserialis on the basis of morphology, embryology, and experimental breeding. *Can. J. Zool.* **70**, 1258-1263.

Shimeld, S. M. (1999). The evolution of the hedgehog gene family in chordates: insights from amphioxus hedgehog. *Dev.t Genes Evol.* **209**, 40-47.

Smith, C. M. and Weisblat, D. A. (1994). Micromere fate maps in leech embryos: lineage-specific differences in rates of cell proliferation. *Development* **120**, 3427-3438.

Song, M. H., Huang, F. Z., Chang, G. Y. and Weisblat, D. A. (2002). Expression and function of an even-skipped homolog in the leech *Helobdella robusta*. *Development* **129**, 3681-3692.

Sukegawa, A., Narita, T., Kameda, T., Saitoh, K., Nohno, T., Iba, H., Yasugi, S. and Fukuda, K. (2000). The concentric structure of the developing gut is regulated by Sonic hedgehog derived from endodermal epithelium. *Development* **127**, 1971-1980.

Tabata, T. and Kornberg, T. B. (1994). Hedgehog is a signaling protein with a key role in patterning Drosophila imaginal discs. *Cell* **76**, 89-102.

Taipale, J., Chen, J. K., Cooper, M. K., Wang, B., Mann, R. K., Milenkovic, L., Scott, M. P. and Beachy, P. A. (2000). Effects of oncogenic mutations in Smoothened and Patched can be reversed by cyclopamine. *Nature* **406**, 1005-1009.

Toftgard, R. (2000). Hedgehog signalling in cancer. *Cell Mol. Life Sci.* **57**, 1720-1731.

Valentine, J. W. and Collins, A. G. (2000). The significance of moulting in Ecdysozoan evolution. *Evol. Dev.* **2**, 152-156.

Vervoort, M. (2000). hedgehog and wing development in Drosophila: a morphogen at work? *BioEssays* **22**, 460-468.

Wedeen, C. J. and Shankland, M. (1997). Mesoderm is required for the formation of a segmented endodermal cell layer in the leech Helobdella. *Dev. Biol.* **191**, 202-214.

Wedeen, C. J. and Weisblat, D. A. (1991). Segmental expression of an engrailed-class gene during early development and neurogenesis in an annelid. *Development* **113**, 805-814.

Weisblat, D. A. and Huang, F. Z. (2001). An overview of glossiphoniid leech development. *Can. J. Zool.* **79**, 218-232.

Weisblat, D. A., Kim, S. Y. and Stent, G. S. (1984). Embryonic origins of cells in the leech *Helobdella triserialis*. *Dev. Biol.* **104**, 65-85.

Weisblat, D. A., Zackson, S. L., Blair, S. S. and Young, J. D. (1980). Cell lineage analysis by intracellular injection of fluorescent tracers. *Science* **209**, 1538-1541.

Wolpert, L. (1994). The evolutionary origin of development: cycles, patterning, privilege and continuity. *Development* **Supplement** 79-84.

Yin, Z. and Frasch, M. (1998). Regulation and function of tinman during dorsal mesoderm induction and heart specification in Drosophila. *Dev. Genet.* **22**, 187-200.